Cluster synchronization and spatio-temporal dynamics in networks of oscillatory and excitable Luo-Rudy cells

O. I. Kanakov and G. V. Osipov
Department of Radiophysics, Nizhny Novgorod University, Gagarin Avenue, 23, 603950 Nizhny Novgorod, Russia

C.-K. Chan
Institute of Physics, Academia Sinica, 128 Sec. 2, Academia Road, Nankang, Taipei 115, Taiwan

J. Kurths
Institute of Physics, University of Potsdam, 19 Am Neuen Palais, D-14415 Potsdam, Germany

(Received 15 September 2006; accepted 3 January 2007; published online 30 March 2007)

We study collective phenomena in nonhomogeneous cardiac cell culture models, including one- and two-dimensional lattices of oscillatory cells and mixtures of oscillatory and excitable cells. Individual cell dynamics is described by a modified Luo-Rudy model with depolarizing current. We focus on the transition from incoherent behavior to global synchronization via cluster synchronization regimes as coupling strength is increased. These regimes are characterized qualitatively by space-time plots and quantitatively by profiles of local frequencies and distributions of cluster sizes in dependence upon coupling strength. We describe spatio-temporal patterns arising during this transition, including pacemakers, spiral waves, and complicated irregular activity. © *2007 American Institute of Physics*. [DOI: 10.1063/1.2437581]

Processes of generation and propagation of cell excitation waves in cardiac tissues are a matter of topical interest because of their importance for understanding normal and pathological types of heart activity. The dynamics of heart tissues has been studied quite extensively in recent years, both experimentally and by means of numerical modeling. A special class of studies is concerned with cardiac cell cultures—thin layers of cells grown in Petri dishes. Characteristic features of such systems are spontaneous oscillatory activity, spatial inhomogeneity and variability of intercellular coupling strength due to an increasing number of cell junctions. The present paper is devoted to modeling the dynamics of spatio-temporal patterns of excitation in such inhomogeneous cultures in dependence upon the coupling strength. The model of a culture is based on the paradigmatic Luo-Rudy model of an isolated cardiac cell. The results of modeling are interpreted in terms of synchronization theory. In particular, cluster synchronization regimes are studied, in which the ensemble of cells gets split into several subgroups (clusters), each characterized by its own oscillation frequency. Several available experimental results (formation of target and spiral waves in cultures) are reproduced by modeling.

I. INTRODUCTION

Modeling biological systems such as neuronal ensembles, kidney, and cardiac tissues is one of the most rapidly developing fields of application of nonlinear dynamics nowadays. The efficiency of these methods is conditioned by the complex, though deterministic behavior of individual cells constituting the tissue.

In particular, cardiac cells exhibit properties of either excitable or oscillatory systems. The former case is observed in working myocardium, and the latter is found in natural cardiac pacemakers (sinoatrial and atrioventricular nodes, Purkinje fibers). Normal heart activity is controlled by waves of excitation generated in the sinoatrial node and propagating through the conducting system and working myocardium. Deviations from the normal regime (arrhythmias) are often associated with pathological types of wave dynamics in the cardiac tissue. They include spiral waves and spiral chaos (the latter manifests itself in heart fibrillation). Significant scientific efforts have been taken to understand these regimes and develop a way of controlling them.[1–6]

In the present paper we report a series of numerical experiments with one- and two-dimensional cardiac cell culture models, including inhomogeneous ensembles of oscillatory cells and mixtures of oscillatory and excitable cells. Individual cell dynamics is described by a modified Luo-Rudy model with depolarizing current. We focus mainly on the transition from incoherent behavior of uncoupled cells to global synchronization in ensembles of strongly coupled cells, when the coupling coefficient is increased from zero. This corresponds to the increase of the number of gap-junctions in the culture.

We show, that this transition occurs via cluster synchronization regimes. We describe spatio-temporal patterns arising during this transition, including pacemakers, spiral waves, and complicated irregular activity. These dynamical effects emerge due to spatial discreteness and inhomogeneity of the model.

Similar experiments *in vitro* were reported in Ref. 7. According to Ref. 7, after approximately 24 h of culture time, irregular spontaneous activity arises in the culture, and

it further organizes itself into several pacemakers emitting target waves. These pacemakers are subsequently destroyed, and spiral wave activity sets in; the number of spiral cores is changing with time.[7]

II. THE MODEL

A. Excitable cells

As a basis, we use the Luo-Rudy phase I model[8] to define the dynamics of a single cell. This model describes the dynamics of excitable cardiac cells and is defined by a system of eight ordinary differential equations (ODE). The first of them is the charge conservation equation

$$C_m\dot{v} = -(I_{\mathrm{Na}} + I_{si} + I_K + I_{K_1} + I_{Kp} + I_b), \tag{1}$$

where v is the membrane voltage measured in millivolts, $C_m = 1\ \mu\mathrm{F/cm}^2$ is the membrane capacity. The time unit is 1 ms. The ionic transmembrane currents in the right-hand part are sodium current, slow inward current (carried by calcium ions), potassium current, inward-rectifier potassium current, plateau potassium current, and background Ohmic current, measured in $\mu\mathrm{A/cm}^2$. They are defined by the following expressions:

$$I_{\mathrm{Na}} = G_{\mathrm{Na}} \cdot m^3 hj \cdot (v - E_{\mathrm{Na}}), \quad I_{si} = G_{si} \cdot df \cdot (v - E_{si}(v,c))$$

$$I_K = G_K \cdot xx_i(v) \cdot (v - E_K), \quad I_{K_1} = G_{K_1} \cdot k_{1i}(v) \cdot (v - E_{K_1}), \tag{2}$$

$$I_{K_p} = G_{K_p} \cdot k_p(v) \cdot (v - E_{K_1}), \quad I_b = G_b \cdot (v - E_b).$$

Here G_q and E_q with $q \in \{\mathrm{Na}, si, K, K_1, K_p, b\}$ denote the maximal conductance and reversal potential of the corresponding ionic current. The gating variables $g_i \in \{m,h,j,d,f,x\}$, $i = 1,\ldots,6$, are governed each by an ODE of the type

$$\dot{g}_i = \alpha_{g_i}(v)(1 - v) - \beta_{g_i}(v)v. \tag{3}$$

The 12 nonlinear functions $\alpha_{g_i}(v)$ and $\beta_{g_i}(v)$ as well as $E_{si}(v,c)$, $x_i(v)$, $k_{1i}(v)$, $k_p(v)$ are fitted to experimental data.[8] The dynamics of the internal calcium ion concentration c is described by an ODE of the first order

$$\dot{c} = 10^{-4} I_{si}(v,d,f,c) + 0.07(10^{-4} - c). \tag{4}$$

The eight ODEs (1), (3), and (4) form a closed system for the variables of state v,m,h,j,d,f,x,c.

The values of the constant parameters are the same as used in Ref. 2.

This model lacks many details taken into account in other models, which are much more complicated.[9–12] However, it still demonstrates good qualitative and quantitative agreement with available experimental data on single-cell dynamics,[8] as opposed to other paradigmatic but more qualitative models like the FitzHugh-Nagumo model.

B. Oscillatory cells and cell cultures

To describe the oscillatory activity of a cell, we modify the model by adding a constant depolarizing current to the ionic currents in (1). We model a two-dimensional cell culture by a square lattice with local diffusive coupling. This type of coupling represents electrical intercellular conductance coupling via gap junctions. The charge conservation equation for a lattice then reads

$$C_m\dot{v}_{ij} = -(I_{\mathrm{Na}} + I_{si} + I_K + I_{K_1} + I_{Kp} + I_b) + I_{ij}^d + D\Delta_d(v_{ij}), \tag{5}$$

where i,j are lattice indices, $I_{ij}^d > 0$ is a constant depolarizing current which is nonidentical in different cells, D is the coupling coefficient, and Δ_d is the second-order central difference operator (discrete Laplacian). A one-dimensional modification of this model is obtained by dropping the second spatial index.

When the value of I_d in an isolated cell is increased above a bifurcation value approximate equal to 2.21 at the chosen values of parameters, a limit cycle appears in the phase space of the model, thus the cell becomes oscillatory. Though this approach might not account for real physiological mechanisms of cell oscillation, the development of a more adequate model is hindered by the lack of understanding of the mentioned mechanisms in *in vitro* experiments. However, in real situations, it is known that the leakage (depolarization) current of the nonpacemaker cells can increase turning them into oscillatory cells when they are dissociated from the heart tissues.[13]

The measured dependence of the oscillation frequency of the cell upon the value of the depolarizing current I^d is presented in Fig. 1.

Note that the spatial scale of one cell in the lattice model corresponds to the characteristic scale of culture inhomogeneity rather than to the size of a single cardiac cell.

III. ONE-DIMENSIONAL MODELS

To get insight into some basic mechanisms, we start with a one-dimensional (1D) version of the model (5). We consider two different settings. In the first one the chain consists purely of oscillatory cells, and in the second one it is a mixture of oscillatory and excitable cells.

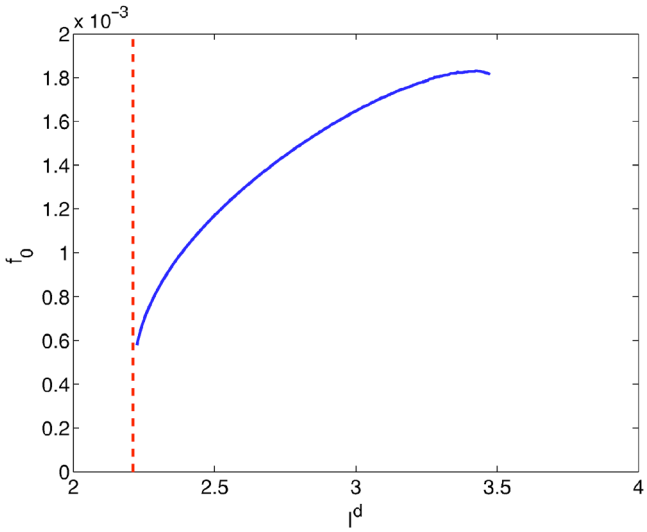

FIG. 1. Frequency of oscillations of an isolated Luo-Rudy cell vs the constant depolarizing current I^d.

A. Ensembles of oscillatory cells

First, we study a chain of $N=400$ oscillatory cells with different natural oscillation frequencies. For this we use quenched random depolarizing currents I_i^d, uniformly distributed in the interval $[2.4;3.2]$ $\mu A/cm^2$. We simulate the total of ten chains with different realizations of this random distribution. The initial conditions are chosen to be identical in each cell, so that all cells in the chain initially get depolarized simultaneously.

We simulate the system dynamics on the interval of 8×10^5 time units. Within this interval, we allow for a transient time of $T_{tr}=4\times10^5$ units for the transient processes to be over and a stationary regime to set in. The duration of T_{tr} is chosen in a way that its further increasing does not lead to changes in the measurement results. In the subsequent observation time of $T_{ob}=4\times10^5$ units we measure the individual average oscillation frequencies of each element. For that we define the section plane for the ith element as $v_i=v_s$, $\dot{v}_i>0$, $v_s=-30.0$, and register each crossing of the trajectory with each of these section planes. We estimate the average oscillation frequency of the ith element as $f_i=(n_i-1)/\Delta t_i$, where n_i is the number of crossings registered for the ith element, and Δt_i is the time elapsed between the first and the last crossing.

In Fig. 2(a) we plot the frequencies f_i of all elements in a chain with one realization of the random distribution of I_i^d versus D with dots. We see, that global synchronization sets in with increasing D, and the transition to global synchronization occurs via cluster regimes. A cluster regime is represented by a set of separated dots for a given value of D (say, $D=0.006$). Each such dot corresponds to a frequency cluster.

In Figs. 3(a)–3(d) we plot the frequency profiles f_i versus element number i for several values of the coupling coefficient D in the same chain. We observe, that the size of clusters is gradually increasing, leading to a global synchronization regime [Fig. 3(d)], when all observed frequencies are equal up to the numerical estimation accuracy.

In Figs. 4(a)–4(d) we present the corresponding space-time color code plots of voltage in the chain, taken after the waiting time of 8×10^5 units. We observe a pacemaker (a local source of waves) in each cluster. A pacemaker is associated with a column of local minima of color lines on a space-time plot. In the global synchronous regime only one pacemaker remains.

We observe a qualitatively similar behavior for all ten tested realizations of the random quenched depolarizing current.

For a more detailed study of cluster synchronization in the system, we introduce its quantitative measure as the ratio of the maximal cluster size in the system N_c to the total

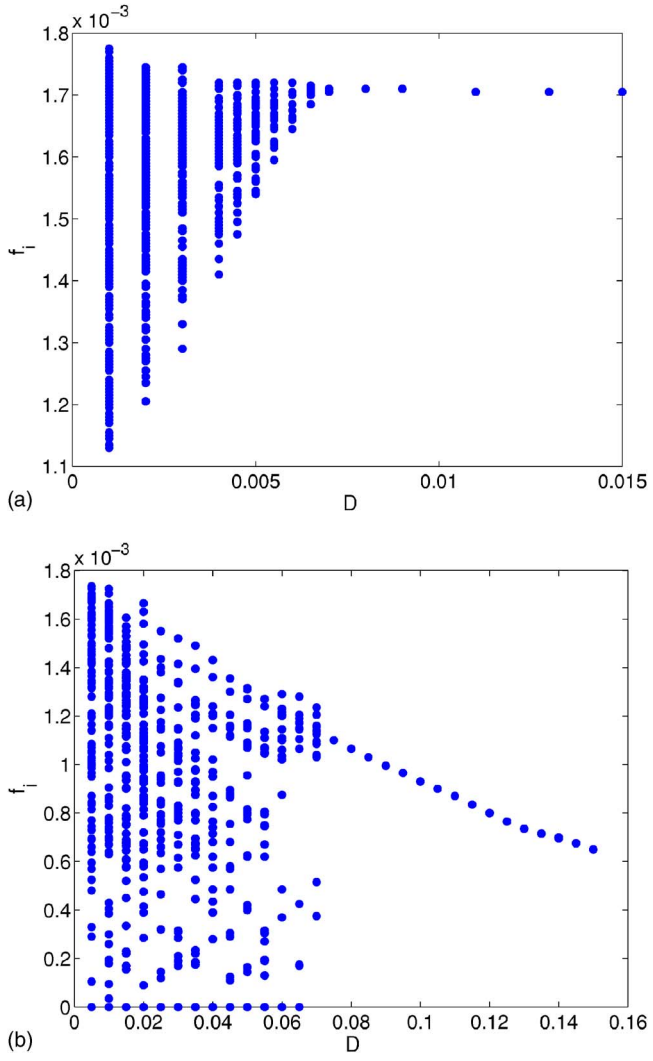

FIG. 2. Distribution of measured oscillation frequencies in a chain of $N=400$ Luo-Rudy cells vs coupling coefficient D. Quenched random depolarizing currents I_i^d are distributed uniformly on the interval $[2.4;3.2]$ (a) and $[0;3.2]$ (b).

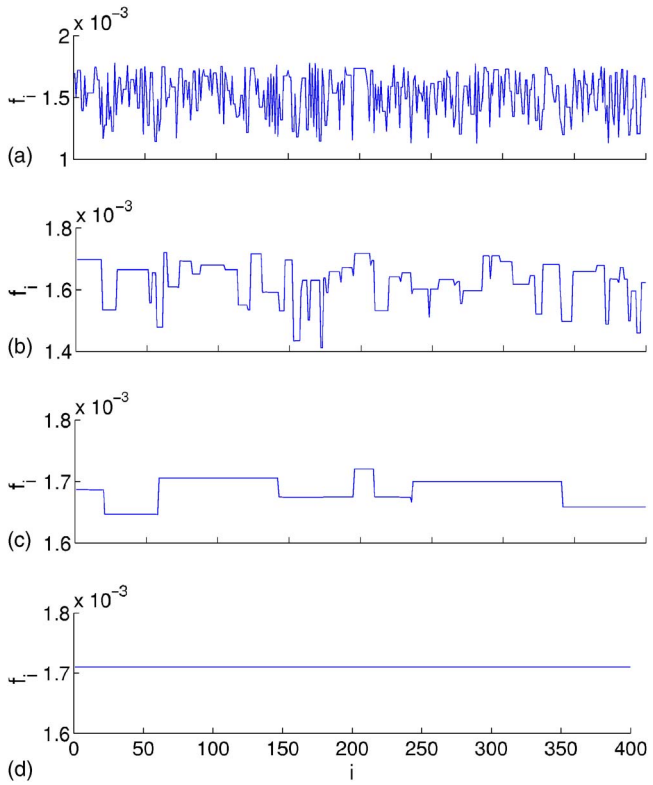

FIG. 3. Measured oscillation frequencies in the oscillatory chain vs cell number i at different values of the coupling coefficient $D=0.001$ (a), 0.004 (b), 0.006 (c), 0.008 (d).

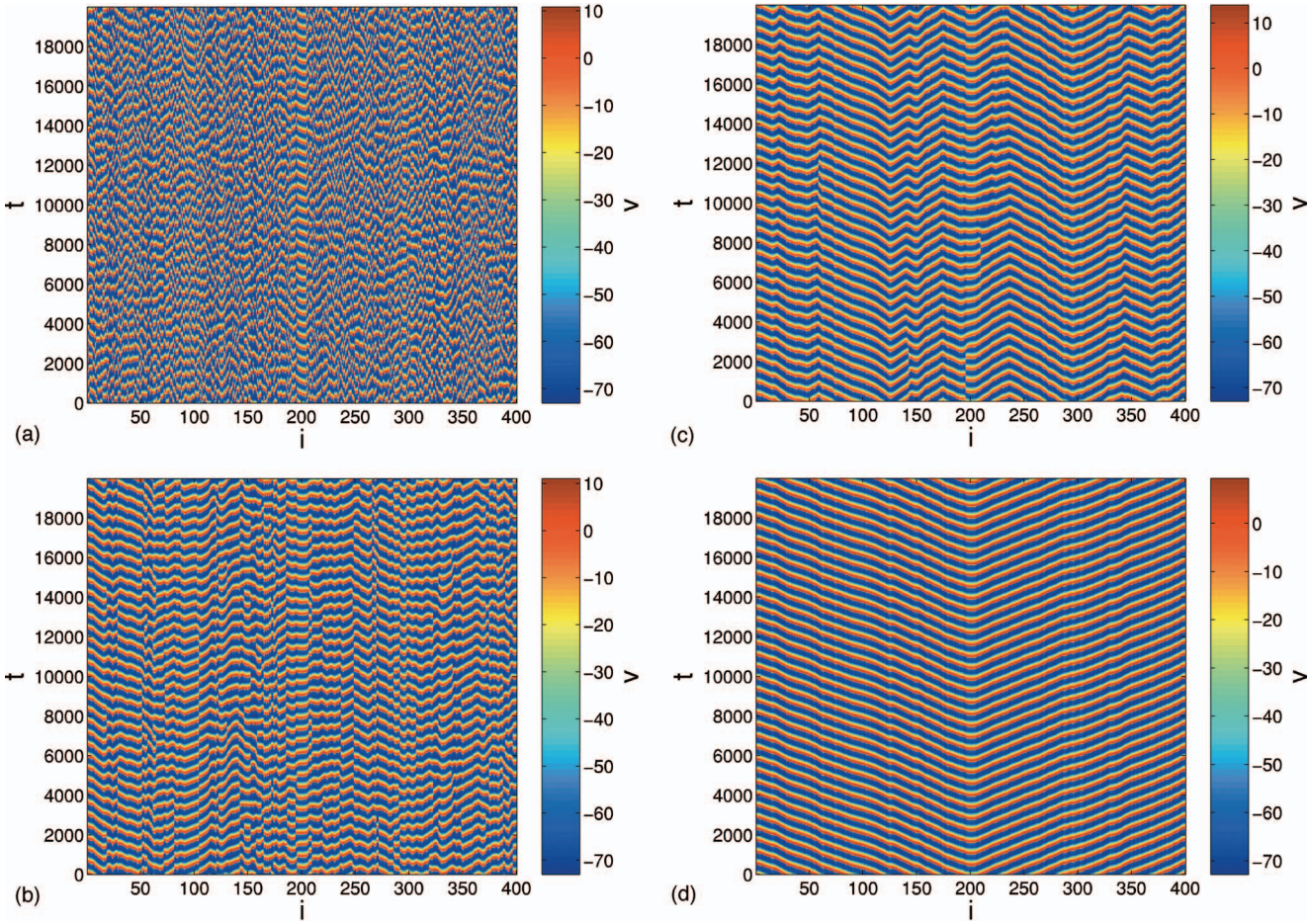

FIG. 4. (Color) Space-time plots of membrane voltage v in the oscillatory chain after waiting time 8×10^5 units at different values of the coupling coefficient $D=0.001$ (a), 0.004 (b), 0.006 (c), 0.008 (d).

system size N. The global synchronization regime thus corresponds to $N_c/N=1$. We define a cluster as a set of adjacent cells with measured average frequencies falling within the same error interval of size defined as $\Delta f=2/T_{\mathrm{ob}}$. In this measurement $\Delta f=5\times10^{-6}$. We plot the ratio N_c/N for ten realizations of the depolarizing current in Fig. 5(a). We observe the ratio generically growing with D, ultimately reaching the value 1. The points falling out of the bulk are due to the randomness in the simulations.

B. Mixtures of oscillatory and excitable cells

Next, we consider a chain which consists of a mixture of excitable and oscillatory Luo-Rudy cells. As heart tissue contains both types of cells, the problem of their interaction was actively studied.[14–17] To obtain a model of a mixture we change the interval of uniform distribution of the depolarizing currents to [0;3.2]. From the numerically found value of the bifurcation point in I^d we conclude, that about 31% of cells are oscillatory when uncoupled, and the other cells are excitable. We perform the same computational analysis of the model as in the previous setting.

We plot average frequencies of all elements in a chain with one realization of the random distribution of I_i^d versus D in Fig. 2(b). The only visible qualitative difference from the case of purely oscillatory chain is that the range of observed frequencies is now starting from zero. Note that the transition to global synchronization occurs at a higher value of D than in the oscillatory case.

Next, we plot the frequency profiles f_i versus cell number i for several values of the coupling coefficient D in the same chain in Figs. 6(a)–6(d). As expected, at small coupling the chain contains narrow groups of oscillating cells, separated by groups of cells at rest, which may be coined zero-frequency clusters (this means in fact, that the driving from neighboring cells is not enough for them to get membrane voltage above v_s). As coupling is increased, the nonzero frequency clusters are typically growing at the expense of zero-frequency ones. Note, that adjacent clusters with frequencies related as small natural numbers (like 1:2 or 2:3) are sometimes observed, see Figs. 6(b) and 6(c). This means, that the propagation of a certain fraction of the pulses (each second or each third in the mentioned examples) from the pacemaker into these regions is suppressed. Like in the case of purely oscillatory system, ultimately the regime of global synchronization sets in [see Fig. 6(d)].

The ratio N_c/N for ten realizations of the depolarizing current is plotted in Fig. 5(b). This ratio is generically growing with increasing D, reaching the value 1 at higher values of D, than in the case of purely oscillatory chain.

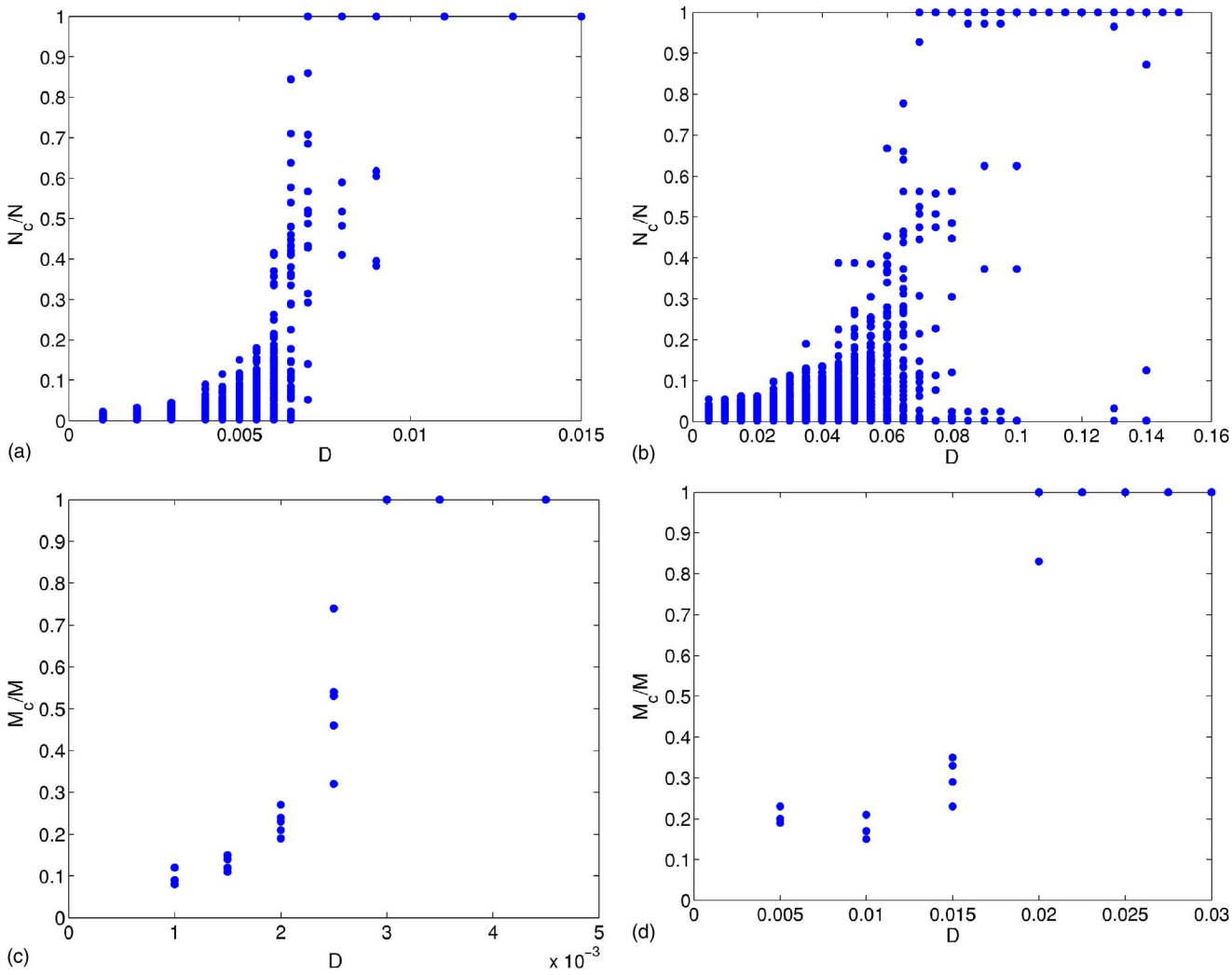

FIG. 5. Size of the largest cluster of synchronization related to the total system size vs coupling coefficient D: [(a) and (b)] in chains of $N=400$ cells for ten different realizations of the uniform random distribution of I_i^d in the intervals [2.4;3.2] (a) and [0;3.2] (b); [(c) and (d)] in lattices of $N=M\times M$ cells, $M=100$, for 5 and 4 different realizations of the same two distributions, respectively.

We also plot the fraction N_z/N of nonexcited (zero-frequency) cells for ten realizations of I^d, see Fig. 7(a). As expected, this fraction is falling from about 0.7 down to zero.

We also carried out simulations of a chain with the depolarizing currents distributed according to the Gaussian law with its mean value equal to 2.8 and standard deviation equal to 0.5. The same qualitative results were reproduced. The transition to global synchronization occurs around $D=0.03$.

IV. TWO-DIMENSIONAL MODELS

In this section we show, that the main results obtained from the 1D models are kept in 2D models as well.

We consider a square lattice of $N=M\times M$, $M=100$, Luo-Rudy cells (5) with the same two distributions of quenched random depolarizing currents as in the 1D case. We perform simulations with five different realizations for the case of purely oscillatory system, and with four realizations for a mixture of oscillatory and excitable cells. The initial conditions are the same as in the 1D case.

The total simulation time interval is 8×10^5 time units. As the transient processes appear to be longer in the 2D case than in the 1D one, we choose transient time $T_{\mathrm{tr}}=6\times 10^5$ units, and observation time $T_{\mathrm{ob}}=2\times 10^5$ units.

Similar to the 1D case, the transition to global synchronization occurs via cluster synchronization regimes. We measure the maximal cluster size M_c in horizontal and vertical directions in a way analogous to that taken in the 1D case. The frequency error interval is taken as $\Delta f=2/T_{\mathrm{ob}}=1\times 10^{-5}$. The ratio M_c/M is plotted in Fig. 5(c) and is qualitatively similar to that obtained in the 1D model. However, now $M_c/M=1$ does not imply global synchronization, because local frequency defects are possible (see below).

Figure 8 shows the measured average oscillation frequency profiles for one realization of the quenched random current distribution on the interval [2.4; 3.2] at four different values of the coupling coefficient D along with corresponding snapshots of membrane voltage v_{ij} in the end of 8×10^5 units time interval. At small coupling $D=0.001$, frequency clusters are formed, but consist of no more than a few cells, and the activity in the lattice looks incoherent [Figs. 8(a) and 8(b)]. As coupling D is increased, the clusters get larger [Figs. 8(c) and 8(d)]. After further increasing D, almost the

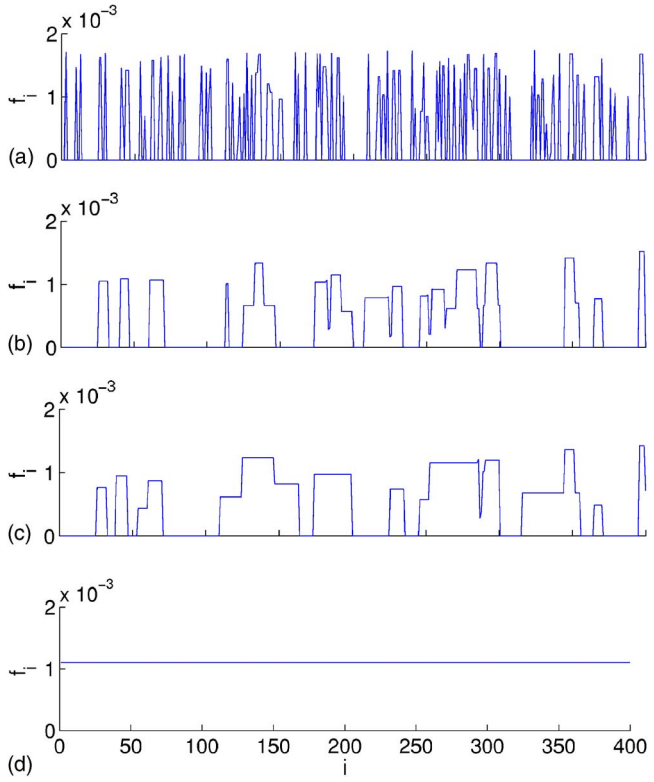

FIG. 6. Measured oscillation frequencies in the chain with oscillatory and excitable elements vs cell number i at different values of the coupling coefficient $D=0.005$ (a), 0.03 (b), 0.04 (c), 0.075 (d).

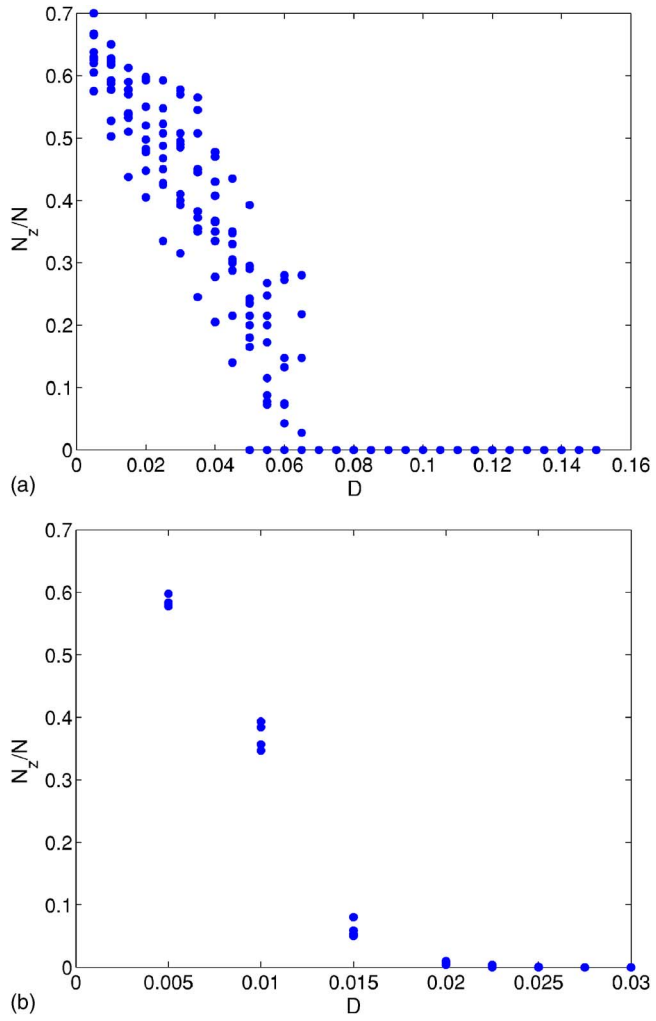

FIG. 7. Number N_z of nonexcited elements related to the total system size N vs coupling coefficient D: (a) in chains of $N=400$ cells for ten different realizations of the uniform random distribution of quenched depolarizing currents I_i^d in the interval [0;3.2]; (b) in lattices of $N=M\times M$ cells, $M=100$, for four different realizations of the same distribution.

whole lattice gets covered with one cluster, except for small "defects" characterized by differing frequencies [Figs. 8(e) and 8(f)]. The corresponding space-time evolution in the latter case is an almost regular target wave structure, but it contains defects in the forms of additional pacemakers and spiral cores, which can coexist [Fig. 8(f)]. Such structural defects and the mentioned defects in the frequency profiles are typically well associated with each other [compare Figs. 8(e) and 8(f)].

Further increasing the coupling parameter leads to a globally synchronous regime. We observe, that it can be represented as well by one pacemaker, two pacemakers and a spiral wave in different realizations of I^d distribution [Figs. 9(a)–9(c), respectively]. However, it is impossible to determine with computational methods, whether two pacemakers indeed do coexist and are frequency-locked, or the finite transient time is insufficient to observe one of them being destroyed, and the observation time in not enough to resolve their frequency difference.

The ratio M_c/M for four realizations of the mixture of oscillatory and excitable cells is plotted versus D in Fig. 5(d), the ratio of the number of nonexcited elements to the total number of elements is presented in Fig. 7(b). We observe that with increasing D, frequency clusters are growing and the fraction of never excited elements is falling to zero. The space-time evolution is characterized by a transition from spatially-incoherent behavior to globally synchronous regimes driven by pacemakers or spirals.

V. DISCUSSIONS

We have studied the dynamics of one- and two-dimensional inhomogeneous cardiac culture models in two settings: (i) an ensemble of oscillatory cells with different natural frequencies and (ii) a mixture of excitable and oscillatory cells. In all these kinds of models we observed the transition from incoherent behavior to global synchronization via cluster synchronization regimes when the coupling strength is increased. We have measured the main quantitative characteristics of these regimes (distributions of local average frequencies and cluster sizes) in dependence upon the coupling strength. In two-dimensional models we observed various spatio-temporal patterns of activity, including target and spiral waves and complicated irregular behavior.

From the consideration above it is clear that the coupling constant D plays an important role in the collective dynamics of the cells. In real situations, this D corresponds probably to the gap-junction connectivity between cells. In an experiment with cardiac cell cultures from chicken embryos, Glass *et al.* have recently shown that the control of connectivity of

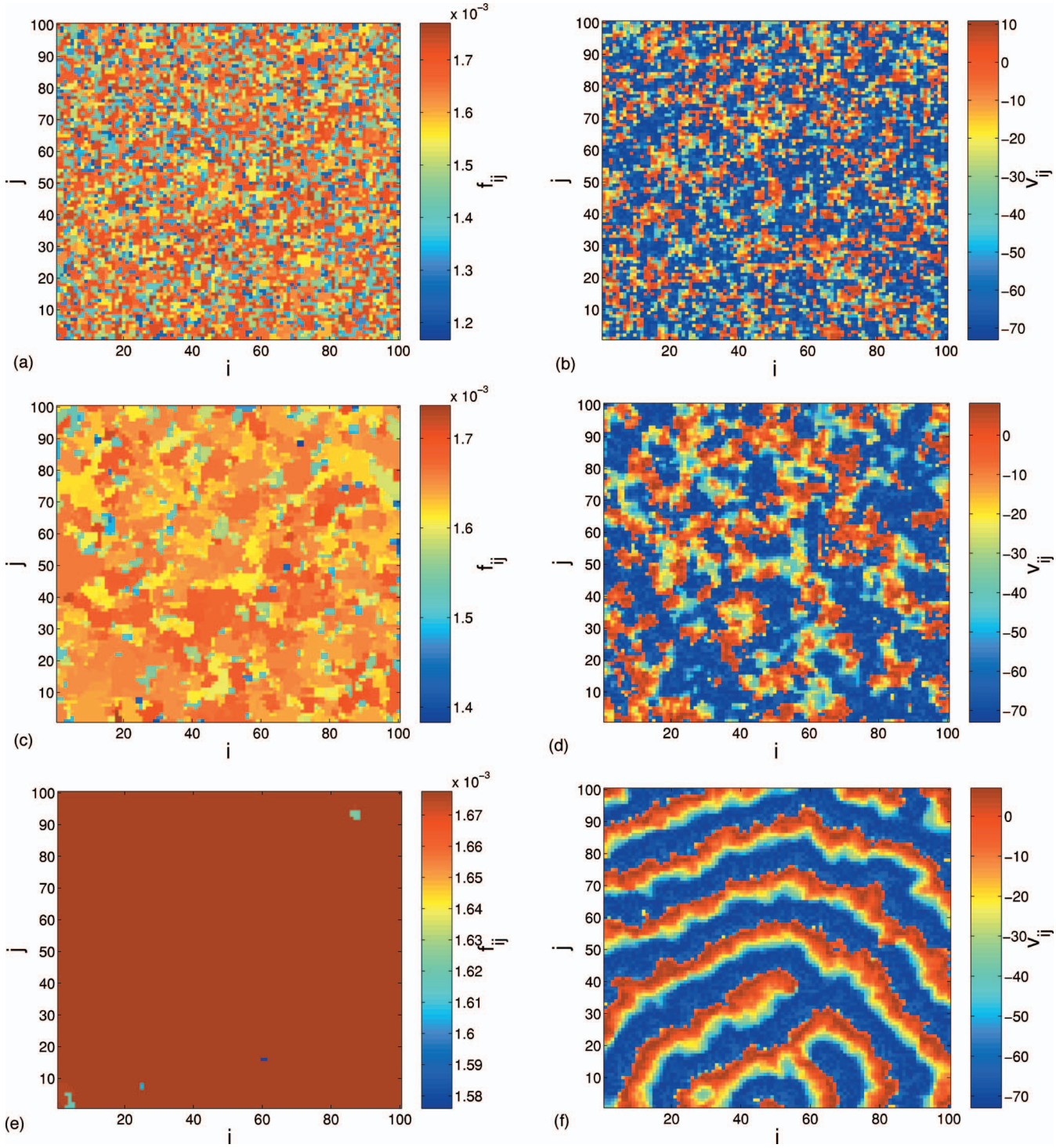

FIG. 8. (Color) Measured oscillation frequencies [(a), (c), and (e)] and snapshots of membrane voltage after waiting time 8×10^5 units [(b), (d), and (f)] in a 2D lattice of 100×100 oscillatory Luo-Rudy cells at different values of the coupling coefficient $D=0.001$ [(a) and (b)], 0.002 [(c) and (d)], $D=0.003$ [(e) and (f)]. Quenched random depolarizing currents I_{ij}^{d} are distributed uniformly on the interval [2.4; 3.2].

the system through the use of α glycerrhetinic acid and cultures density can indeed produce a transition to synchronized patterns.[18] They have used a heterogeneous cellular automaton model to understand their experiment findings. It seems that heterogeneity and excitability are essential in their explanations.

In our case, the system is oscillatory or is a mixture of excitable and oscillatory cells. Although cells taken from the ventricle[7] are considered to be only excitable when they are in an intact heart, they will become oscillatory[13] after they have been dissociated from the heart tissue and plated on the culture dishes. It is known that their oscillation period will be much longer than that of the pacemakers, but it is not clear what the oscillation period distribution is and whether this distribution will depend on the growth conditions. Even though all the cells might eventually be oscillatory, as a first

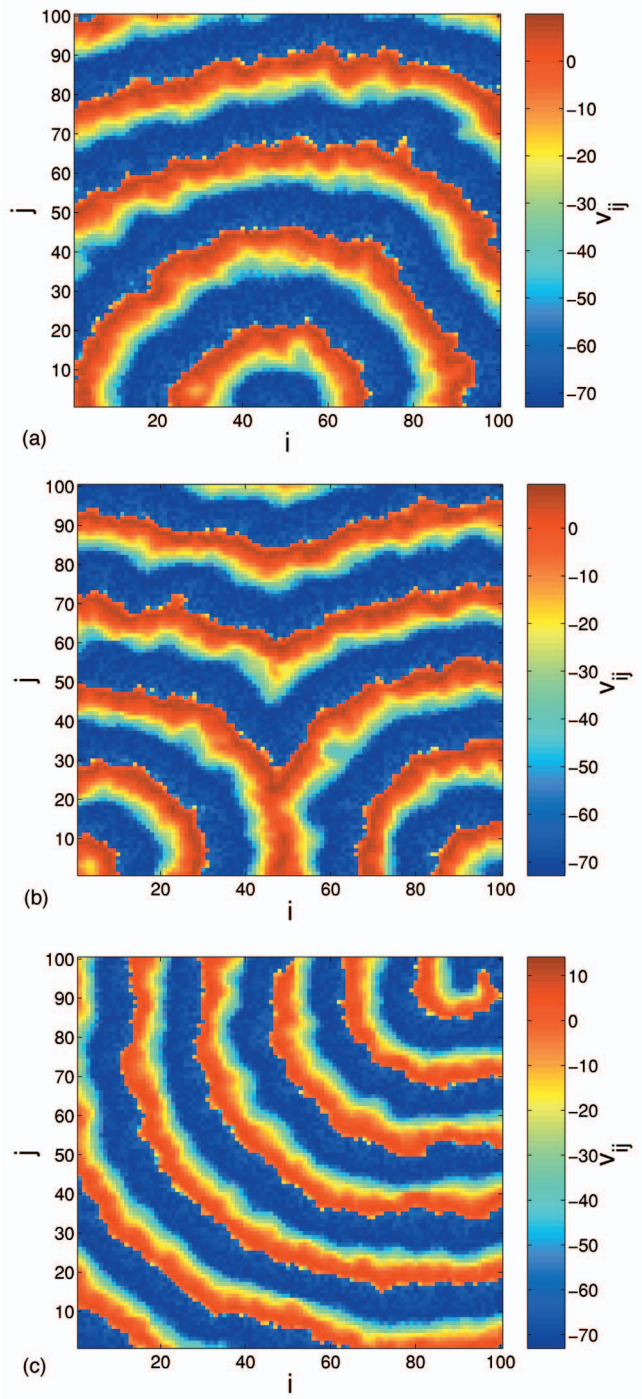

FIG. 9. (Color) Snapshots of membrane voltage after waiting time 8×10^5 units in a 2D lattice of 100×100 oscillatory Luo-Rudy cells for four different realizations of the uniform random distribution of quenched depolarizing currents I_{ij}^d at $D=0.004$. In all cases global synchronization up to numerical accuracy is observed.

approximation, one can still consider most of the cells as excitable as they will be driven by a few cells with the shortest oscillation periods. It is therefore reasonable to assume that there is a mixture of excitable and oscillatory cells. In this sense, we also have heterogeneity and excitability built into our systems. However, the question is open whether this heterogeneity is the same as that of Glass *et al.*[18]

ACKNOWLEDGMENTS

This research was supported by RFBR-NSC (Project No. 05-02-90567), RFBR-MFC (Project No. 05-02-19815), RFBR (Project Nos. 06-02-16596 and 06-02-16499) and the program "Leading Scientific Schools of Russia" (Grant No. 7309.2006.2). O.I.K. also acknowledges support from the "Dynasty" Foundation, Russia, and J.K. that of the International Promotionskolleg Cognitive Neuroscience and BIOSIM.

[1] V. I. Krinsky, "Spread of excitation in an inhomogeneous medium," Biophysics (Engl. Transl.) **11**, 776–784 (1966).
[2] A. T. Stamp, G. V. Osipov, and J. J. Collins, "Suppressing arrhythmias in cardiac models using overdrive pacing and calcium channel blockers," Chaos **12**, 931–940 (2002).
[3] J. N. Weiss, Z. Qu, P. S. Chen, S. F. Lin, H. S. Karagueuzian, H.Hayashi, A.Garfinkel, and A.Karma, "The dynamics of cardiac fibrillation," Circulation **112**, 1232–1240 (2005).
[4] H. Zhang, Zh.Cao, N.-J. Wu, H.-P. Ying , and G. Hu, "Suppress Winfree turbulence by local forcing excitable systems," Phys. Rev. Lett. **94**, 188301 (2005).
[5] Focus issue: "Fibrillation in normal ventricular myocardium," Chaos **8**, 1–241 (1998).
[6] Focus issue: "Mapping and control of complex cardiac arrhythmias," Chaos **12**, 732–981 (2002).
[7] S.-M. Hwang, K.-H. Yea, and K. J. Lee, "Regular and alternate spiral waves of contractile motion on rat ventricle cell cultures," Phys. Rev. Lett. **92**, 198103 (2004).
[8] C.-H. Luo and Y. Rudy, "A model of the ventricular cardiac action potential: Depolarization, repolarization, and their interaction," Circ. Res. **68**, 1501–1526 (1991).
[9] C.-H. Luo and Y. Rudy, "A dynamic model of the cardiac ventricular action potential. I. Simulations of ionic currents and concentration changes," Circ. Res. **74**, 1071–1096 (1994).
[10] M. Courtemanche, R. J. Ramirez, and S. Nattel, "Ionic mechanisms underlying human atrial action potential properties: Insights from a mathematical model," Am. J. Physiol. **275**, H301–H321 (1998).
[11] K. H. Ten Tusscher, D. Noble, P. J. Noble, and A. V. Panfilov, "A model for human ventricular tissue," Am. J. Physiol. Heart Circ. Physiol. **286**, H1573–H1589 (2004).
[12] K. H. Ten Tusscher and A. V. Panfilov, "Alternans and spiral breakup in a human ventricular tissue model," Am. J. Physiol. Heart Circ. Physiol. **291**, H1088–H1100 (2006).
[13] S. L. Lilly, *Pathophysiology of Heart Disease*, 3rd ed. (Lippincott, Williams, and Wilkins, New York, 2003).
[14] H. A. Fozzard and M. Schoenberg, "Strength—duration curves in cardiac Purkinje fibres: Effects of laminal length and charge distribution," J. Physiol. (London) **226**, 593–618 (1972).
[15] R. L. Winslow, A. Varghese, D. Noble, C. Adlakha, and A.Hoythya, "Generation and propagation of ectopic beats induced by spatially localized Na-K pump inhibition in atrial network models," Proc. R. Soc. London, Ser. B **254**, 55–61 (1993).
[16] R. W. Joyner, Y. G. Wang, R. Wilders, D. A. Golod, M. B. Wagner, R. Kumar, and W. N. Goolsby, "A spontaneously active focus drives a model atrial sheet more easily than a model ventricular sheet," Am. J. Physiol. **279**, H752–H763 (2000).
[17] R. Wilders, M. B. Wagner, D. A. Golod, R. Kumar, Y. G. Wang, W. N. Goolsby, R. W. Joyner, and H. J. Jongsma, "Effects of anisotropy on the development of cardiac arrhythmias associated with focal activity," Pfluegers Arch. **441**, 301–302 (2000).
[18] G. Bub, A. Shrier, and L. Glass, "Global organization of dynamics in oscillatory heterogeneous excitable media," Phys. Rev. Lett. **94**, 028105 (2005).